

Multivariant synthesis, crystal structures and properties of four nickel coordination polymers based on flexible ligands

Sheng-Quan Lu,^a Kang Fang,^a Yong-Yao Liu,^a Ming-Xing Li,^a Sui-Jun Liu,^{c*}

Xiang He^{ab*}

a Department of Chemistry, College of Sciences, Shanghai University, Shanghai, China, 200444.

b State Key Laboratory of Structural Chemistry, Fujian Institute of Research on the Structure of Matter, Chinese Academy of Sciences, Fuzhou, Fujian 350002, China.

c School of Metallurgy and Chemical Engineering, Jiangxi University of Science and Technology, Ganzhou, Jiangxi Province, China, 341000.

* Corresponding author. E-mail: hxiang@shu.edu.cn; liusuijun147@163.com

Contents

Table S1. Selected bond distances (\AA) and angles ($^{\circ}$) for compounds **1-4**.

Table S2. The different products of different metal-ligand-bpe ratio.

Table S3. The different products of different pH at the ratio of metal-ligand-bpe is 1:2:1.

Table S4. The different products of different solvent ratio (NMP/H₂O).

Figure S1. The PXRD partterns of product from DMA/H₂O system and compound **4**.

Table S5. Crystallographic data for compound **3'**.

Table S6. Selected bond distances (\AA) and angles ($^{\circ}$) for compound **3'**.

Figure S2. Conversion of compound **4** into **3**.

Figure S3. The topology net of **2**.

Figure S4. a) The 1D cation chain of $[\text{Ni}_{0.5}(\text{bpe})_{0.5}(\text{H}_2\text{O})_2]_n^{n+}$ in **3**, b) The two-fold interpenetrating architecture $[\text{Ni}(\text{L})(\text{bpe})(\text{H}_2\text{O})]_n^{n-}$ constituted from 2D layers in **3**.

Table S7. The dihedral angels and torsion angels of the H₃L ligand in Compounds **1-4**

Table S8. The dihedral angels and torsion angels of the bpe in Compounds **1-4**

Figure S5. The FT-IR Spectra of H₄L ligand and compounds **1-4**.

Figure S6. The PXRD patterns of compounds **1-4** and the simulated spectra.

Figure S7. TGA-DTA curves for **1-4**.

Scheme S1. Schematic representation of magnetic mode in **2**.

Table S1. Selected bond distances (\AA) and angles ($^\circ$) for compounds **1-4**

Compound 1					
N(1)-Ni(1)	2.131(4)	O(9)-Ni(2)-N(2)#4	94.02(13)	O(1)-Ni(1)-N(1)	93.75(13)
N(2)-Ni(2)#1	2.107(4)	O(3)-Ni(2)-O(9)	91.41(12)	O(1)#2-Ni(1)-N(1)	86.25(13)
Ni(1)-O(1)	2.032(3)	O(1)#2-Ni(1)-O(8)	88.14(12)	O(8)-Ni(1)-N(1)	90.93(14)
Ni(1)-O(8)	2.096(3)	O(9)-Ni(2)-O(9)#3	180.0	O(8)#2-Ni(1)-N(1)	89.07(14)
Ni(2)-O(3)	2.048(3)	O(3)-Ni(2)-N(2)#4	90.55(14)	N(1)-Ni(1)-N(1)#2	180.00(18)
Ni(2)-O(9)	2.084(3)	O(3)#3-Ni(2)-O(9)	88.59(12)	O(9)#3-Ni(2)-N(2)#4	85.98(13)
O(1)-Ni(1)-O(8)	91.86(12)	O(3)-Ni(2)-O(3)#3	180.00(16)	O(3)#3-Ni(2)-N(2)#4	89.45(14)
O(1)-Ni(1)-O(1)#2	180.0				

Symmetry transformations used to generate equivalent atoms: #1 x,y-1,z, #2 -x+1,-y,-z, #3 -x+1,-y+1,-z+1, #4 -x+1,-y,-z+1, #5 x,y+1,z for **1**.

Compound 2					
N(1)-Ni(1)	2.103(5)	O(9)#2-Ni(1)-O(1)	94.53(14)	O(6)#3-Ni(1)-N(2)#1	86.81(17)
N(2)-Ni(1)#1	2.136(4)	O(9)#2-Ni(1)-O(6)#3	90.43(15)	O(4)#2-Ni(1)-N(2)#1	85.37(15)
Ni(1)-O(9)#2	1.994(3)	O(1)-Ni(1)-O(6)#3	89.74(16)	N(1)-Ni(1)-N(2)#1	93.05(19)
Ni(1)-O(1)	2.057(4)	O(9)#2-Ni(1)-O(4)#2	95.23(13)	O(2)#4-Ni(2)-O(2)	90.8(2)
Ni(1)-O(6)#3	2.065(4)	O(1)-Ni(1)-O(4)#2	169.81(15)	O(2)#4-Ni(2)-O(9)#2	173.46(14)
Ni(1)-O(4)#2	2.069(4)	O(6)#3-Ni(1)-O(4)#2	87.23(16)	O(9)-Ni(3)-O(7)#6	88.35(14)
Ni(2)-O(2)#4	2.048(4)	O(9)#2-Ni(1)-N(1)	89.74(17)	O(9)#2-Ni(2)-O(8)	87.08(15)
Ni(2)-O(9)#2	2.052(3)	O(1)-Ni(1)-N(1)	93.11(17)	O(9)#2-Ni(2)-O(9)#5	81.23(19)
Ni(2)-O(8)	2.103(4)	O(6)#3-Ni(1)-N(1)	177.11(17)	O(2)#4-Ni(2)-O(8)	88.99(17)
Ni(3)-O(9)	2.042(3)	O(4)#2-Ni(1)-N(1)	89.89(17)	O(9)-Ni(3)-O(3)	96.71(14)
Ni(3)-O(3)	2.084(3)	O(9)#2-Ni(1)-N(2)#1	177.15(17)	O(3)-Ni(3)-O(3)#4	85.2(2)
Ni(3)-O(7)#6	2.091(4)	O(1)-Ni(1)-N(2)#1	84.75(15)	O(3)-Ni(3)-O(7)#6	89.10(14)
O(8)-Ni(2)-O(8)#4	173.4(2)	O(9)-Ni(3)-O(9)#4	81.72(18)	O(9)#4-Ni(3)-O(7)#6	95.52(14)

Symmetry transformations used to generate equivalent atoms: #1 -x+1/2,y,-z+1/2, #2 x,y-1,z, #3 -x+1,-y+1,-z+1, #4 -x+3/2,y,-z+1/2, #5 -x+3/2,y-1,-z+1/2, #6 x+1/2,-y+2,z-1/2, #7 -x+1,-y+2,-z+1, #8 x,y+1,z for **2**.

Compound 3					
N(1)-Ni(1)	2.070(3)	O(3)#3-Ni(1)-O(5)	98.89(9)	O(3)#3-Ni(1)-N(2)#4	90.23(10)
N(2)-Ni(1)#2	2.086(3)	O(3)#3-Ni(1)-N(1)	87.86(10)	O(5)-Ni(1)-N(2)#4	92.79(10)
N(5)-Ni(2)	2.081(3)	O(5)-Ni(1)-N(1)	87.85(10)	N(1)-Ni(1)-N(2)#4	178.06(10)
Ni(1)-O(3)#3	2.021(2)	O(3)#3-Ni(1)-O(1)	160.82(9)	O(5)-Ni(1)-O(1)	100.25(9)
Ni(1)-O(5)	2.054(2)	N(1)-Ni(1)-O(1)	91.84(10)	N(2)#4-Ni(1)-O(1)	89.86(10)
Ni(1)-O(1)	2.099(2)	O(3)#3-Ni(1)-O(2)	99.66(9)	O(5)-Ni(1)-O(2)	161.42(8)
Ni(1)-O(2)	2.202(2)	N(1)-Ni(1)-O(2)	91.92(10)	N(2)#4-Ni(1)-O(2)	88.06(10)
Ni(2)-O(18)#5	2.098(2)	O(17)#5-Ni(2)-O(17)	180.0	N(5)-Ni(2)-N(5)#5	180.0
Ni(2)-O(17)#5	2.106(2)	N(5)-Ni(2)-O(18)#5	92.18(10)	O(18)#5-Ni(2)-O(18)	180.0
O(1)-Ni(1)-O(2)	61.18(8)	N(5)-Ni(2)-O(17)#5	87.45(10)	O(18)-Ni(2)-O(17)#5	89.84(11)

Symmetry transformations used to generate equivalent atoms: #1 -x+1,-y+1,-z+1, #2 x,y,z+1, #3 x-1,y,z, #4 x,y,-z-1, #5 -x+1,-y,-z+1, #6 x+1,y,z for **3**.

Compound 4					
N(1)-Ni(1)	2.078(4)	O(3)#2-Ni(1)-O(8)	94.82(15)	O(3)#2-Ni(1)-N(1)	93.32(15)

N(2)-Ni(1)#1	2.085(4)	O(8)-Ni(1)-N(1)	90.00(15)	O(3)#2-Ni(1)-N(2)#3	90.60(15)
Ni(1)-O(3)#2	2.010(3)	O(8)-Ni(1)-N(2)#3	88.92(16)	N(1)-Ni(1)-N(2)#3	176.01(16)
Ni(1)-O(8)	2.075(4)	O(3)#2-Ni(1)-O(2)	159.90(14)	O(8)-Ni(1)-O(2)	104.81(15)
Ni(1)-O(2)	2.127(4)	N(1)-Ni(1)-O(2)	91.00(15)	N(2)#3-Ni(1)-O(2)	85.56(15)
Ni(1)-O(1)	2.132(4)	O(3)#2-Ni(1)-O(1)	98.49(14)	O(8)-Ni(1)-O(1)	166.58(14)
N(1)-Ni(1)-O(1)	90.91(16)	N(2)#3-Ni(1)-O(1)	89.25(16)	O(2)-Ni(1)-O(1)	61.79(13)

Symmetry transformations used to generate equivalent atoms: #1 $x+1,y,z$, #2 $-x,y-1/2,-z+1/2$, #3 $x-1,y,z$, #4 $-x,y+1/2,-z+1/2$ for **4**.

Table S2. The different products of different metal-ligand-bpe ratio

Metal-ligand-bpe Ratio	1:1:1	1:2:1	x:2:1(x≥2)
140°C, 0.2ml 1M NaOH(aq)	3	1	2

Table S3. The different products of different pH at the ratio of metal-ligand-bpe is 1:2:1

Different pH	5.5	~	6.5
140°C	1	1+3	3

Table S4. The different products of different solvent ratio (NMP/H₂O)

Different solvent ratio (NMP/H ₂ O)	0:8	0.5:7.5	2:6	4:4	6:2
140°C	1+amorphous	4+amorphous	4	4+amorphous	amorphous

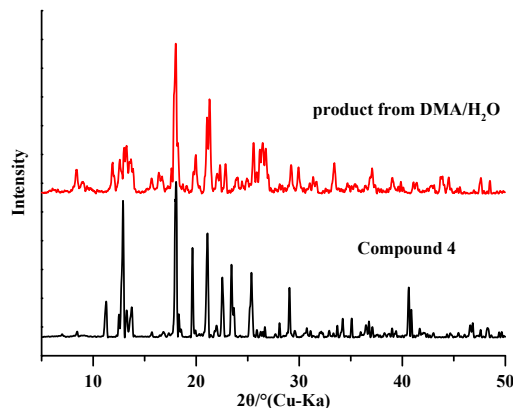


Figure S1. The PXRD parttern of product from DMA/H₂O system and compound **4**.

Table S5. Crystallographic data for compound **3'**

Compound	3'
Formula	C ₃₄ H ₃₅ N ₃ O ₁₁ Ni _{1.5}
Formula weight	749.71
Crystal system	Triclinic
Space group	P-1

$a(\text{\AA})$	10.162(16)
$b(\text{\AA})$	13.36(2)
$c(\text{\AA})$	13.36(2)
$\alpha(^{\circ})$	72.61(3)
$\beta(^{\circ})$	83.85(2)
$\gamma(^{\circ})$	82.09(3)
$V(\text{\AA}^3)$	1710(5)
Z	2
$D_c (\text{g cm}^{-3})$	1.456
$F(000)$	780
GOF on F^2	0.882
$R_1, wR_2 [I > 2\sigma(I)]$	0.0819, 0.1764
R_1, wR_2 (all data)	0.1647, 0.2147
R_{int}	0.0594

Table S6. Selected bond distances (\AA) and angles ($^{\circ}$) for compound **3'**

Compound 3'					
N(1)-Ni(1)	2.107(10)	N(3)#4-Ni(2)-O(10)	92.7(3)	O(8)-Ni(1)-N(1)	92.5(3)
N(2)-Ni(1)#3	2.074(10)	O(10)-Ni(2)-O(10)#4	180.0	N(2)#5-Ni(1)-N(1)	176.7(5)
N(3)-Ni(2)	2.087(10)	N(3)#4-Ni(2)-O(9)	87.6(3)	O(4)-Ni(1)-O(5)#6	161.6(3)
Ni(2)-O(10)	2.094(7)	O(10)-Ni(2)-O(9)	91.1(3)	O(8)-Ni(1)-O(5)#6	99.8(3)
Ni(2)-O(9)	2.098(8)	N(3)#4-Ni(2)-O(9)#4	92.4(3)	N(2)#5-Ni(1)-O(5)#6	92.5(3)
Ni(1)-O(4)	1.992(8)	O(9)-Ni(2)-O(9)#4	180.0	N(1)-Ni(1)-O(5)#6	90.3(4)
Ni(1)-O(8)	2.054(7)	O(4)-Ni(1)-O(8)	98.6(3)	O(4)-Ni(1)-O(6)#6	99.4(3)
Ni(1)-O(5)#6	2.120(8)	O(4)-Ni(1)-N(2)#5	86.6(4)	O(8)-Ni(1)-O(6)#6	162.0(3)
Ni(1)-O(6)#6	2.194(7)	O(8)-Ni(1)-N(2)#5	88.6(3)	N(2)#5-Ni(1)-O(6)#6	92.1(3)
N(3)#4-Ni(2)-N(3)	180.0	O(4)-Ni(1)-N(1)	90.2(4)	N(1)-Ni(1)-O(6)#6	87.8(3)
		O(5)#6-Ni(1)-O(6)#6	62.2(3)		

Symmetry transformations used to generate equivalent atoms: #1 $x+1,y,z$, #2 $-x,-y+2,-z$, #3 $x,y,z+1$, #4 $-x,-y+1,-z$, #5 $x,y,z-1$, #6 $x-1,y,z$, for **3'**.

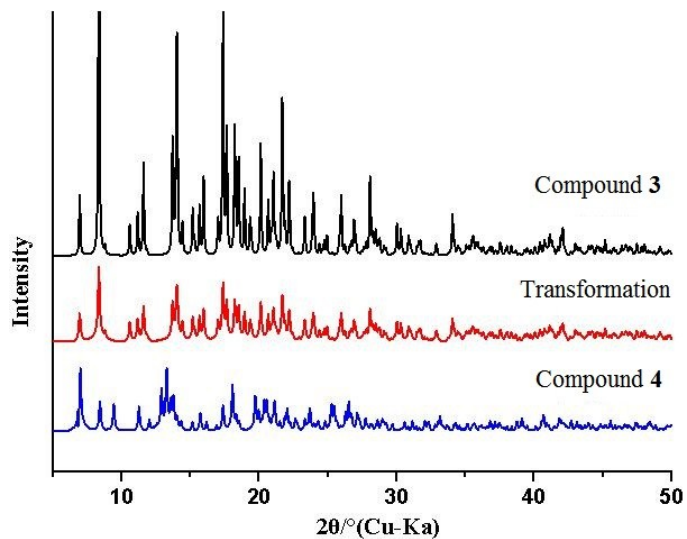


Figure S2. The simulated patterns of compound **3** (top) and compound **4** (bottom), the experimental patterns of **3'** by step-wise synthesis (middle).

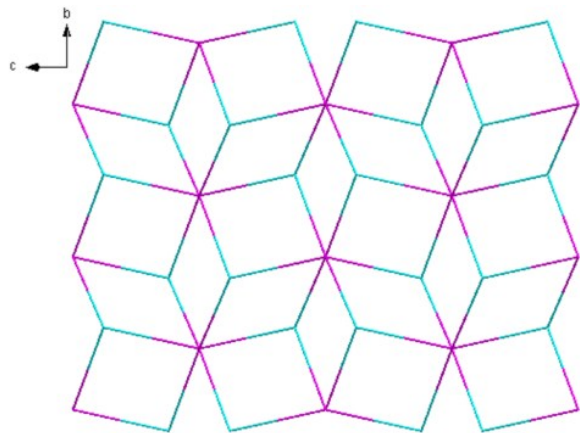


Figure S3. The topology net of **2**.

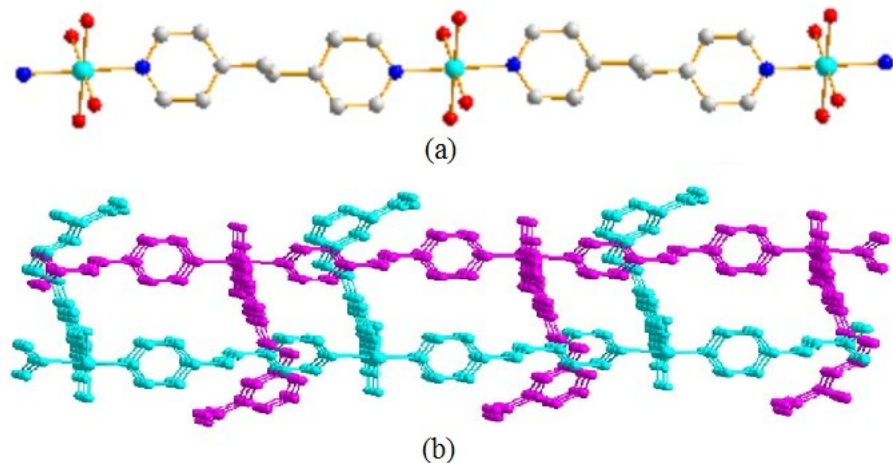


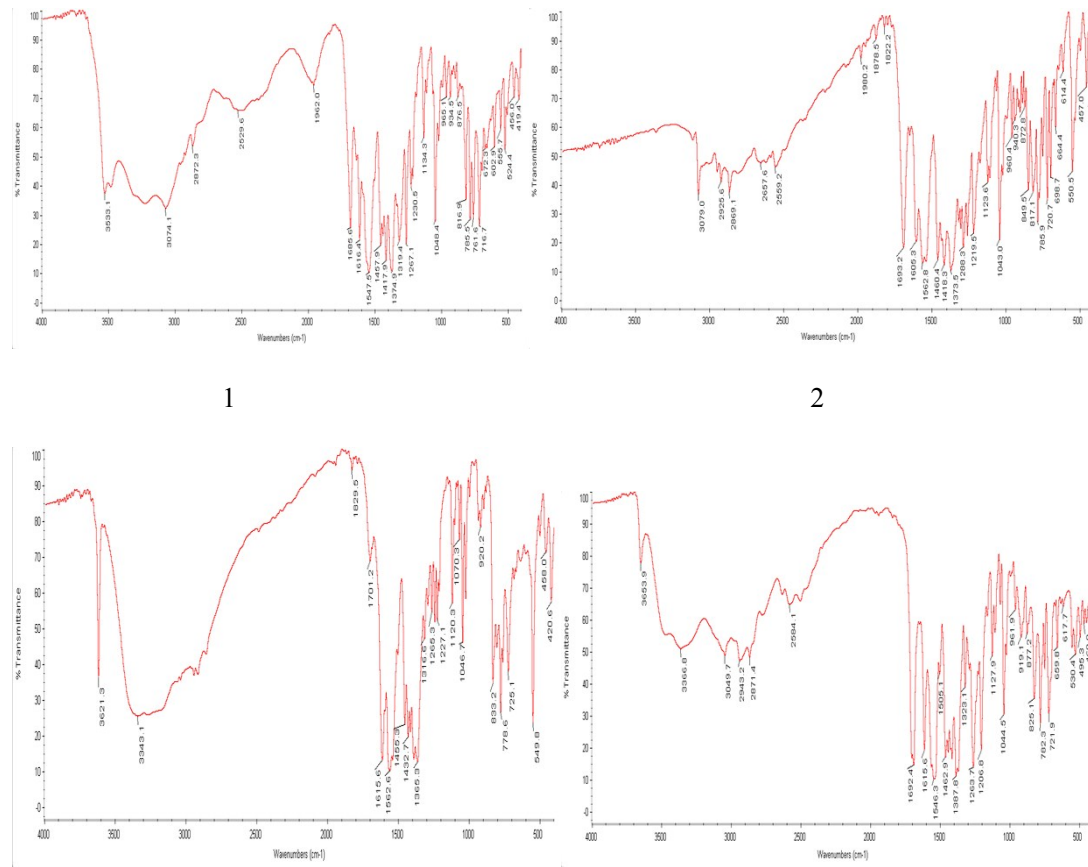
Figure S4. a) The 1D cation chain of $[\text{Ni}_{0.5}(\text{bpe})_{0.5}(\text{H}_2\text{O})_2]^{n+}$ in **3**, b) The two-fold interpenetrating architecture $[\text{Ni}(\text{L})(\text{bpe})(\text{H}_2\text{O})]^{n-}$ constituted from 2D layers in **3**.

Table S7. The dihedral angles and torsion angles of the H₃L ligand in Compounds **1-4**

	dihedral angle (°)	Torsion angle (°)
1	69.872(25)	179.802(69)
2	71.590(11)	-173.615(28)
3	78.222(20)	109.289(50)
4	76.822(5)	-171.468(21)

Table S8. The dihedral angels and torsion angels of the bpe in Compounds **1-4**

	dihedral angle (°)	Torsion angle (°)
1	52.714(25)	55.104(86)
2	46.722(10)	67.013(34)
3 (2D)	28.058(16)	-179.141(39)
3 (1D)	0.000(24)	-180.000(39)
4	47.924(10)	174.81(2)

**Figure S5.** The FT-IR Spectra of H₄L ligand and compounds **1-4**.

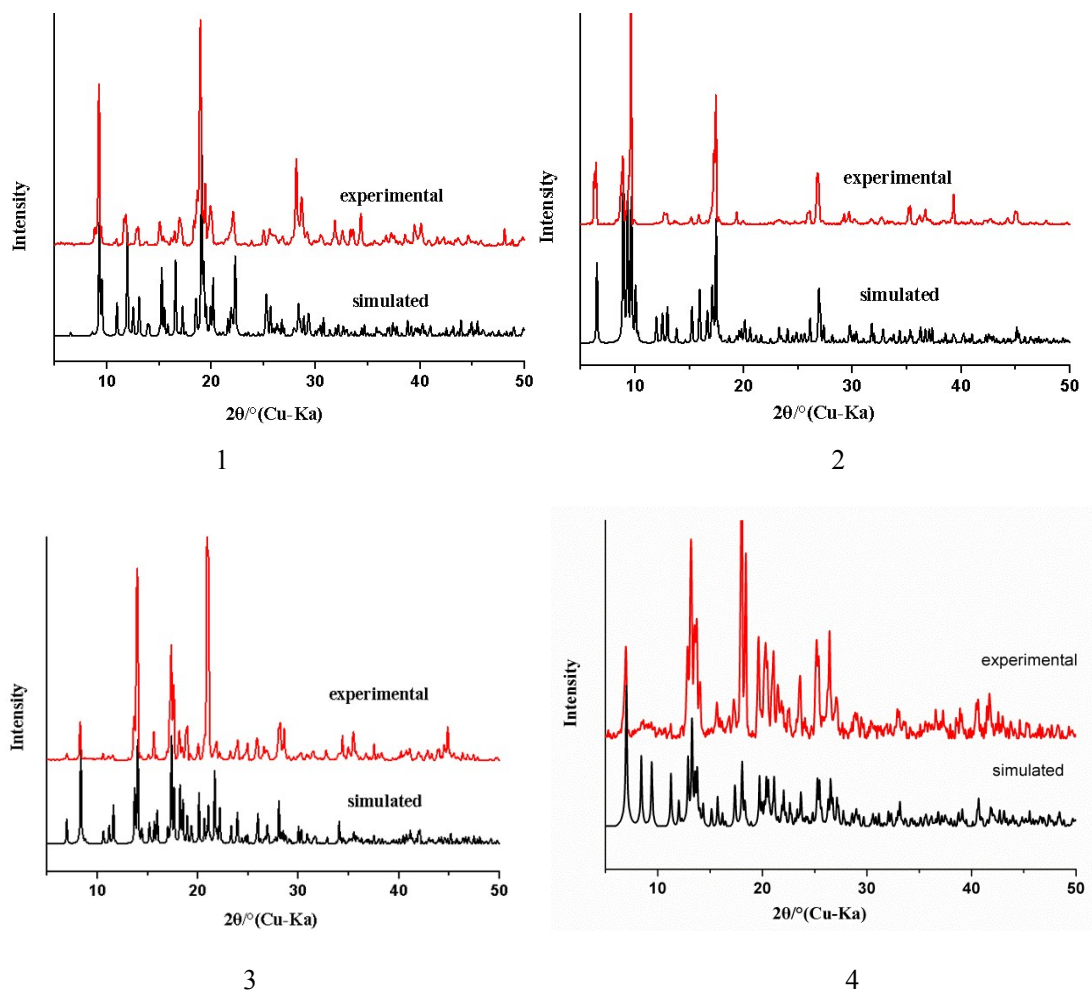
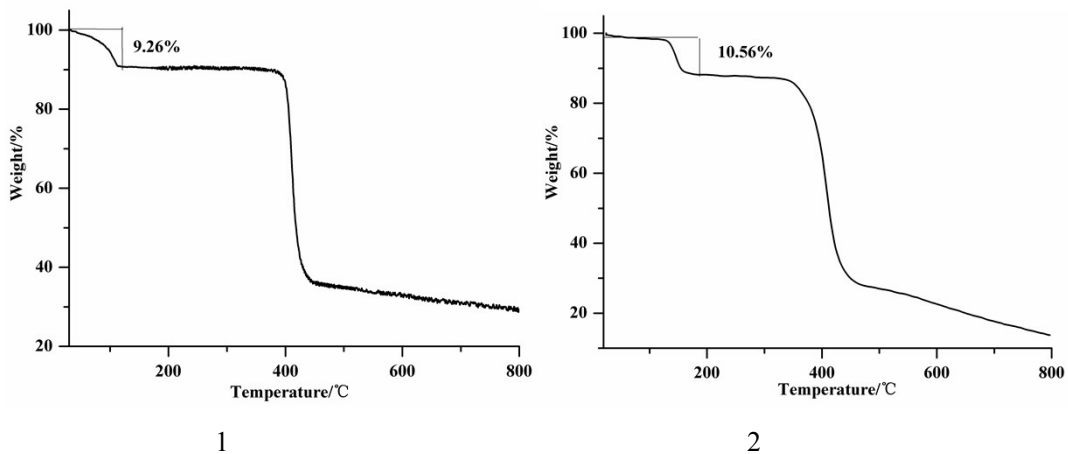
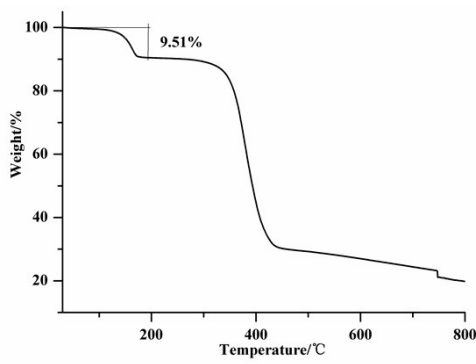
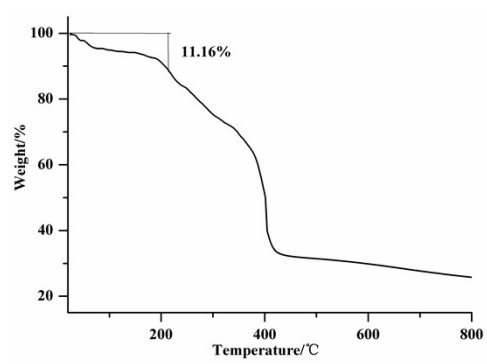


Figure S6. The PXRD patterns of compounds **1-4** and the simulated spectra.



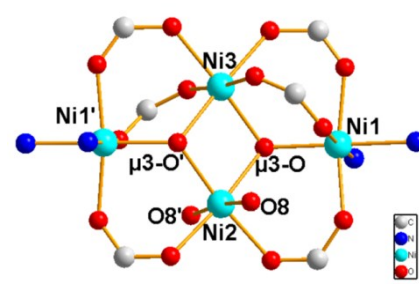
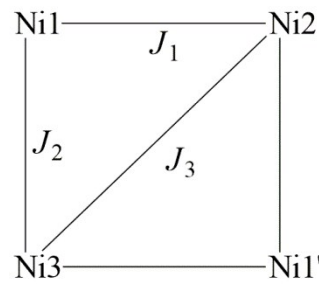


3



4

Figure S7. TGA-DTA curves for **1-4**.



Scheme S1. Schematic representation of magnetic mode in **2**.